This article has been published in the Journal of Composite Structures. Please refer this article as- "Moisture effects on the bending fatigue of laminated composites", M. Meng; H. Le, S. Grove, M. J. Rizvi, Composite Structures, vol. 154, 15 October 2016, pp. 49-60. doi:10.1016/j.compstruct.2016.06.078
[URL: http://www.sciencedirect.com/science/article/pii/S0263822316310807]

Moisture effects on the bending fatigue of laminated composites

Maozhou Meng[1], Huirong Le[2]*, Stephen Grove[1], M. Jahir Rizvi[1]

[1]School of Marine Science and Engineering, Plymouth University, Plymouth, United Kingdom

[2]Department of Engineering, University of Derby, Derby, United Kingdom

Corresponding author: Email: h.le@derby.ac.uk

Abstract

This paper investigated the effect of moisture ingress on the bending fatigue of laminated composites. An accelerated testing method was developed to investigate the interaction between composite fatigue and moisture diffusion effects. Unidirectional and cross-ply laminated CFRP composites were manufactured in autoclave, and then submerged in either fresh or seawater for various periods. Quasi-static and cyclic tests were carried out in both air and wet environment, and the failure mechanisms were investigated using visual and microscopic methods. Additionally, a robust 2D Finite Element model (FEA) was developed to simulate the fatigue crack propagation based on Virtual Crack Closure Technique (VCCT), while a 3D FEA model was developed to investigate the edge effect on fatigue crack propagation. The experimental observations gave a good agreement with the FEA models. The study showed that the bending fatigue failure was due to the so-called buckling-driven delamination, and the fatigue life was reduced significantly owing to the combination of edge effect and capillary effect. Therefore, a 4-step fatigue failure theory was proposed to explain the moisture effects on the crack propagation under bending fatigue.

Keywords: Fatigue, Laminated composites, Buckling-driven delamination, FEA

This article has been published in the Journal of Composite Structures. Please refer this article as- "Moisture effects on the bending fatigue of laminated composites", M. Meng; H. Le, S. Grove, M. J. Rizvi, Composite Structures, vol. 154, 15 October 2016, pp. 49-60. doi:10.1016/j.compstruct.2016.06.078
[URL: http://www.sciencedirect.com/science/article/pii/S0263822316310807]

1. Introduction

Compared with the aerospace industry which relies on the ratio of strength to weight, the use of marine composites was attracted by their superior performance of environmental resistance and fatigue life. Since the FRP composites can be moulded to very complex shape, these materials have been successfully introduced to construct the blades of tidal or underwater turbine [1-3]. The challenges for composite materials used in marine environment include the long exposure time of moisture, temperature, numerous ionic species as well as the microorganisms. Recently, a multiscale study of CFRP composite has been demonstrated that the marine environment exposure not only affects the stress distribution in composite laminates but also degrades the interface of the fibre and matrix [4, 5]. In the marine environment, the mechanical structure is designed to have a service life of several decades, and the determination of the resistance to combined state of cyclic stress is a fundamental problem concerning the marine uses of FRP composites. Therefore environmental fatigue is the main concern of the engineers in design of the marine structures to control the cost of maintenance.

The fatigue of FRP composites in ambient environment had been investigated intensively, in which some of them developed theories to predict the composite fatigue [6-8]. Meanwhile, the marine environmental effects on the durability of FRP composites had been investigated by correlating the exposure time with the decrease of tensile strength [9], fibre/matrix interfacial strength [10], transverse and shear strengths [11, 12]. In view of the complexity of the environmental effects and the damage accumulation during fatigue cycling, there is little hope for including fibre breakage, matrix cracking, interfacial debonding and delamination in a single formula. On the other hand, most of the previous works focused on the uniform axial loads, which neglect some stress components such as out-of-plane stresses. Due to the nature of bending, laminates are subjected to tension, compression and shear, which is fundamentally different from the uniaxial loads [13]. However, there have been few reports on the environmental effects on the bending fatigue.

Many mathematical techniques have been developed to predict the crack growth, in which some of the most popular methods used for the delamination of composites are extended finite element method (XFEM) [14-16], cohesive element method (CZM) [17, 18] and virtual crack closure technique (VCCT) [19-21]. The advantage of XFEM, predicting the onset of the crack by maximum principal stress/strain, is commonly combined with the other methods to model the crack initiation and propagation. However, the fracture criterion of XFEM is based on tensile strength which is unlikely to predict the onset of the crack in bending correctly because the composite is subject to compression delamination.

The present work was intended to understand how the moisture diffusion affects the failure mechanisms of laminated composites in bending fatigue. Unidirectional ($[0]_{16}$) and cross-ply ($[90/0]_{4s}$) laminates were manufactured and tested in bending fatigue following ISO standards

This article has been published in the Journal of Composite Structures. Please refer this article as- "Moisture effects on the bending fatigue of laminated composites", M. Meng; H. Le, S. Grove, M. J. Rizvi, Composite Structures, vol. 154, 15 October 2016, pp. 49-60. doi:10.1016/j.compstruct.2016.06.078
[URL: http://www.sciencedirect.com/science/article/pii/S0263822316310807]

[22, 23] to perform the flexural behaviour and ASTM standard [24] to simulate marine environmental exposure. A robust 2D FEA model based on VCCT was then applied to examine the buckling-driven delamination in bending fatigue, while a 3D FEA model was applied to investigate the free edge effects and the effects of water ingress. The mode I and mode II strain energy release rates in critical areas of the laminated composites were examined and correlated with the observation of the fatigue crack propagation in experiments.

2. Experimental methods

2.1 Material preparation

Unidirectional (UD) and cross-ply (CP) laminates made up of pre-preg CFRP composites (Cycom HTS/977-2) were used for the study. This is a high temperature (180°C) curing toughened epoxy resin with 212°C glass transition temperature (Tg) which is formulated for autoclave moulding. The pre-preg CFRP composite plates were autoclave-manufactured and sliced into the designated dimension ($length \times width = 100mm \times 15mm$) following the ISO standards [22, 23].

Table 1 Quasi-static bending test results (apparent flexural strength) and their standard deviations (SDs). The apparent flexural strength was calculated with the 'large-deflection correction' provided by ISO standard [13].

	Immersion*	$\sigma_x^{app}(MPa)$	
		Dry	Saturation
UD($[0]_{16}$)	Sea	1598±56	1696±41
	SP		1780±122
	Tap		1688±137
CP($[90/0]_{4s}$)	Sea	1416±53	1441±40
	SP		1398±88
	Tap		1400±74

***'Sea': sea water immersion; 'Tap': tap water immersion; 'SP': sea water immersion with 70bar hydrostatic pressure**

The coupons were divided into two sets: (a) the as-received (dry) coupons were tested in quasi-static 3-point bending in the normal environment following the ISO standard [22], and the apparent flexural strength was recorded for the criterion to define the loading level for the bending fatigue tests. Some of the as-received coupons were saved for the fatigue test; (b) the second set of coupons were submerged in three chambers which contained fresh water, sea water and sea water with 70bar hydrostatic pressure respectively. In order to accelerate the diffusion process, all the three chambers were placed in an oven at a constant temperature of 50°C. The coupons were saturated after soaking for three months, and then the flexural strength was measured in quasi-static 3-point bending in ambient condition and was

This article has been published in the Journal of Composite Structures. Please refer this article as- "Moisture effects on the bending fatigue of laminated composites", M. Meng; H. Le, S. Grove, M. J. Rizvi, Composite Structures, vol. 154, 15 October 2016, pp. 49-60. doi:10.1016/j.compstruct.2016.06.078
[URL: http://www.sciencedirect.com/science/article/pii/S0263822316310807]

compared with that of un-soaked coupons. After moisture saturation, some of the immersed coupons were saved for the fatigue test. The quasi-static bending test results of both as-received and immersed coupons are shown in Table 1.

2.2 Bending fatigue setup

The bending fatigue, conducted in accordance with ISO standard [23], was carried out on a universal fatigue testing machine (INSTRON E3000) which created a sinusoidal cyclic load. The R ratio (minimum load to maximum load) was fixed at 0.1 and the load control method (constant maximum and minimum forces for each cycle) was applied. The main concern of the choice of frequency was the heat generation and the thermal conductivity (associated with heat dispersion) of the specimen. Since the carbon fibres present much higher value of thermal conductivity than other kinds of fibres, a relatively higher frequency can be applied on a CFRP specimen. Many researchers employed 5 Hz for GFRP composite and 10 Hz for CFRP composites; however 30 Hz for CFRP composites was reported in some cases [25]. According to the FEA simulation (ANSYS Workbench), the first order of resonance frequency of the unidirectional and cross-ply laminates were calculated in the order of 600 Hz and 900 Hz respectively, therefore the resonance effect can be neglected when the loading frequency is in the range of 5-30 Hz. In the present work, most of the specimens were tested at a frequency of 10 Hz though a few were at 15 Hz for comparison.

Table 2 Loading levels of the UD and CP laminates for the fatigue test. The level '100%' represents the ultimate flexural strength which was measured in quasi-static bending. The apparent flexural stresses corresponding to the loading levels are also shown in the table.

This article has been published in the Journal of Composite Structures. Please refer this article as- "Moisture effects on the bending fatigue of laminated composites", M. Meng; H. Le, S. Grove, M. J. Rizvi, Composite Structures, vol. 154, 15 October 2016, pp. 49-60. doi:10.1016/j.compstruct.2016.06.078
[URL: http://www.sciencedirect.com/science/article/pii/S0263822316310807]

	Bending	Level	F_{mean}(N)	F_{amp}(N)	σ_{max}(MPa)
UD $[0]_{16}$	3-Point	65%UFS	305	250	1039
		80%UFS	375	307	1278
		90%UFS	422	345	1438
		100%UFS	853	–	1598
	4-Point	65%UFS	458	374	1039
		80%UFS	563	461	1278
		90%UFS	634	518	1438
		100%UFS	1280	–	1598
CP $[90/0]_{4s}$	3-Point	65%UFS	225	184	924
		80%UFS	277	227	1137
		90%UFS	312	255	1279
		100%UFS	630	–	1421
	4-Point	65%UFS	338	276	924
		80%UFS	416	340	1137
		90%UFS	468	383	1279
		100%UFS	945	–	1421

Specimens were mainly tested at 80% and 90% UFS (ultimate flexural strength), though a few specimens were tested at 65% UFS for comparison. The ultimate flexural strengths of the unidirectional and cross-ply laminates were inherited from the quasi-static bending tests shown in Table 1. The mean value and amplitude are necessary for machine setup, which are calculated by,

$$F_{mean} = \frac{F_{\max}(1+R)}{2}$$
$$F_{amp} = \frac{F_{\max}(1-R)}{2} \qquad (1)$$

with R=0.1. Table 1 has shown that the flexural strengths of the dry and wet specimens were very close to each other; therefore the loading levels for both dry and wet specimens with the same layup were the same in the fatigue tests. Table 2 shows the loading levels corresponding to the mean value and amplitude.

In order to simulate the condition of water immersion, the specimen was covered by a wet sponge which was regularly replenished with water by a tube during the fatigue test, using sea water or tap water on appropriate. Fig.1 shows the three test conditions: Dry-3P, Dry-4P and Wet-4P. The deflection and reaction force at the loading point were recorded.

This article has been published in the Journal of Composite Structures. Please refer this article as- "Moisture effects on the bending fatigue of laminated composites", M. Meng; H. Le, S. Grove, M. J. Rizvi, Composite Structures, vol. 154, 15 October 2016, pp. 49-60. doi:10.1016/j.compstruct.2016.06.078
[URL: http://www.sciencedirect.com/science/article/pii/S0263822316310807]

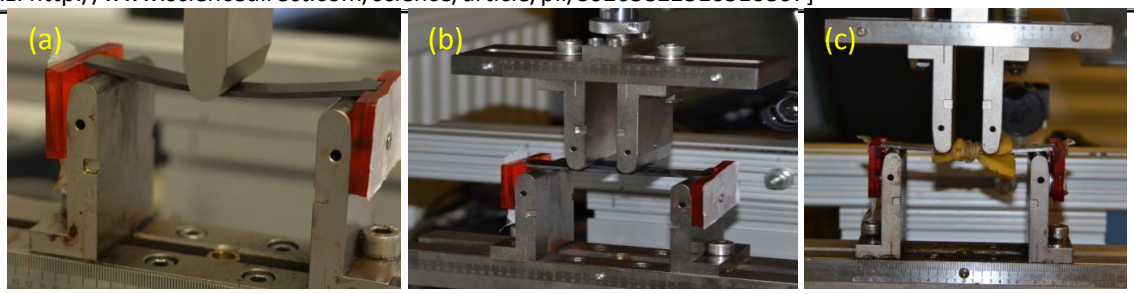

Fig.1. Fatigue test condition: (a) 3-point bending for specimen without immersion (Dry-3P); (b) 4-point bending for specimen without immersion (Dry-4P) and for immersed specimen without the cover of wet sponge (Wet2-4P); and (c) 4-point bending for immersed specimen covered by wet sponge (Wet1-4P).

The machine applied a linear increase of the load to the mean value for five seconds. After that a gradually ramped amplitude cyclic loading sequence was applied until the designated loading level was reached. The fatigue machine showed a variety of responses for unidirectional and cross-ply laminates at the end of the fatigue test, indicating different failure modes. Fig.2 shows the reaction force and deflection of a unidirectional laminate at fracture then the criterion was tripped the limit and the machine stopped. The rapid drop of the reaction force to zero indicated that the specimen failed suddenly and broke into two parts.

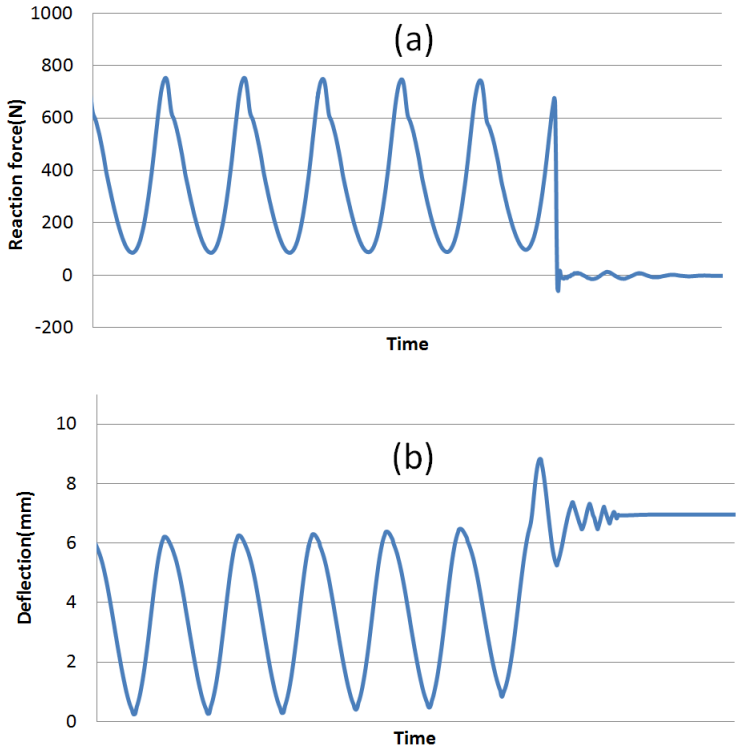

Fig.2. The reaction force (a) and deflection (b) response of a UD specimen at the moment when the specimen broke

This article has been published in the Journal of Composite Structures. Please refer this article as- "Moisture effects on the bending fatigue of laminated composites", M. Meng; H. Le, S. Grove, M. J. Rizvi, Composite Structures, vol. 154, 15 October 2016, pp. 49-60. doi:10.1016/j.compstruct.2016.06.078
[URL: http://www.sciencedirect.com/science/article/pii/S0263822316310807]

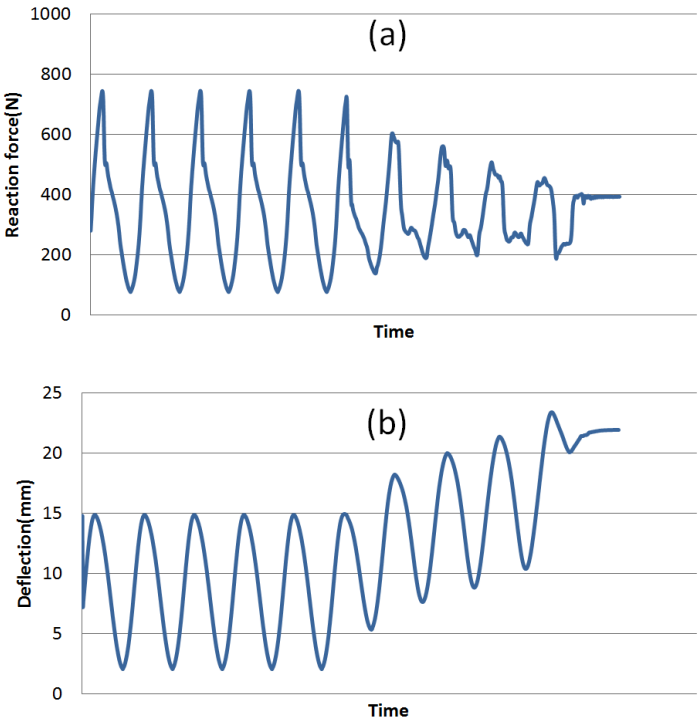

Fig.3. The reaction force (a) and deflection (b) response of a CP specimen at the stage when the specimen broke

Fig.3 shows the reaction force and deflection of a cross-ply laminate when it failed. Instead of the zero reaction force at failure, the deflection increased gradually until the limit was tripped. The machine then stopped automatically while the reaction force remained at a constant level, indicating that the specimen suffered significant fracture but did not break into two parts.

3. Fatigue test results

3.1 Fatigue life

Fig.4 shows the fatigue life of the cross-ply laminate in respect of four testing environments. Some rules can be summarized from these data, though the distribution of the fatigue life at different loading levels and testing environments showed relatively high scatter. At 90% UFS, both wet and dry specimens were tested in 4-point bending and all of the specimens were broken at no more than 10^6 cycles. In the meantime, the immersed specimen showed a lower cycle count than those without immersion. At 80% UFS, all the dry specimens presented infinite fatigue life (more than 3×10^6 cycles) at this testing condition. In contrast, all of the immersed specimens failed. The plot of the fatigue cycle count for the dry specimens scatters at 80% UFS loading level in the figure because the tests were stopped manually when it was found that the fatigue cycle count had exceeded 3×10^6, and such specimens were labelled as

This article has been published in the Journal of Composite Structures. Please refer this article as- "Moisture effects on the bending fatigue of laminated composites", M. Meng; H. Le, S. Grove, M. J. Rizvi, Composite Structures, vol. 154, 15 October 2016, pp. 49-60. doi:10.1016/j.compstruct.2016.06.078
[URL: http://www.sciencedirect.com/science/article/pii/S0263822316310807]

having an infinite fatigue life. It is interesting to notice that the immersed specimen tested without the cover of the wet sponge survived at this loading level, indicating that the fatigue behaviour was also affected by the testing environment. At 65% UFS, all of the specimens survived regardless of the laminate pre-conditions and testing environments.

The unidirectional laminate showed a similar trend at the loading levels, as plotted in Fig.5. At the 90% UFS loading level, no specimen could withstand 3×10^6 fatigue cycles. At the 80% UFS loading level, the dry specimen survived while all the immersed specimens failed. More specifically, as shown in the magnified chart for the immersed specimens at 80% UFS loading level, the cycle counts of the three kinds of water immersions showed such large scatter that there was no clear evidence of any difference of the effects of the three kinds of water immersions on the fatigue life. It had been found that the sea water immersion specimens presented a larger number of bare fibres than tap water condition [5], meaning that the degradation in sea water was more severe than in tap water. One possible explanation for this phenomenon is that the 3-month period of water immersion was not long enough to see the obvious difference of the effects on the fatigue performance. Compared to the cross-ply laminate, the immersed unidirectional specimen broke at 65% UFS, indicating that the effects of water immersion on cut-off fatigue life were dependent on laminate stacking.

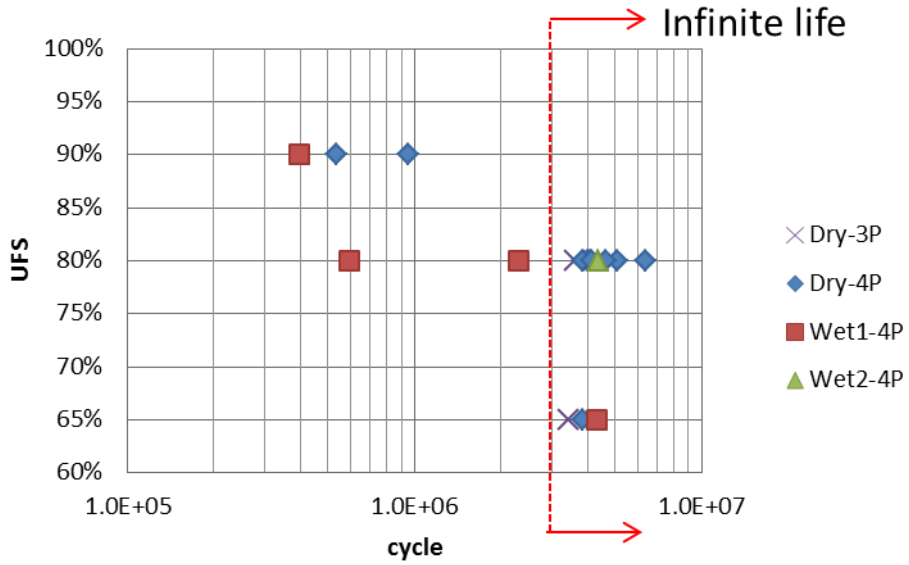

Fig.4. Fatigue life of CP laminate. The fatigue cycle is plotted as logarithm scale. Wet1-4P: immersed specimen, covered by wet sponge while 4-point bending fatigue testing; Wet2-4P: immersed specimen, without wet sponge cover while testing.

This article has been published in the Journal of Composite Structures. Please refer this article as- "Moisture effects on the bending fatigue of laminated composites", M. Meng; H. Le, S. Grove, M. J. Rizvi, Composite Structures, vol. 154, 15 October 2016, pp. 49-60. doi:10.1016/j.compstruct.2016.06.078
[URL: http://www.sciencedirect.com/science/article/pii/S0263822316310807]

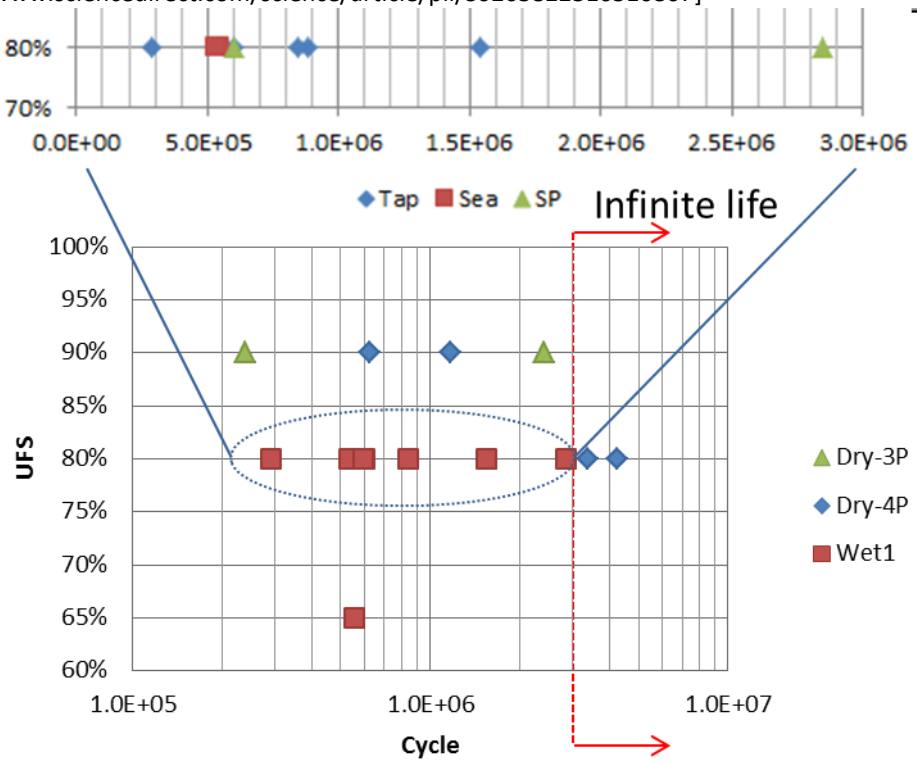

Fig.5. Fatigue life of UD laminate. Tap: tap water immersion; Sea: sea water immersion; SP: sea water immersion with 70 bars hydrostatic pressure.

The fatigue lives of the UD and CP laminates shown in Figs.4 and 5 share many common features, one of which is that the distribution of the ultimate fatigue cycles showed huge scatter. Additionally, these values were extremely high and strongly dependent on the laminate pre-conditions (dry or wet), testing environments as well as the laminate stacking. In fact, the fatigue performance is also dependent on the other factors, such as the bending condition. Therefore it is reasonable to believe that the traditional SN curve, which is widely used to predict the fatigue of metal, is inappropriate to present the fatigue behaviour of FRP composites, and the analysis of their fatigue failure requires consideration of the other aspects, such as the durability of the stiffness during the fatigue test, crack initiation and propagation.

3.2 Fatigue stiffness

The quasi-static bending test had shown a perfect linear force-deflection curve for the simply supported laminate in 3-point and 4-point bending when the ratio of deflection to span was lower than 10% (as in the fatigue cases). The ISO standard [22] provides equations to calculate the apparent flexural modulus for 3-point and 4-point bending,

$$E_{3P}^{f} = \frac{L_{3P}^{3}}{4wh^{3}} \frac{F_{\max}}{D_{\max}}$$
$$E_{4P}^{f} = \frac{0.21L_{4P}^{3}}{wh^{3}} \frac{F_{\max}}{D_{\max}^{mid}} \qquad (2)$$

This article has been published in the Journal of Composite Structures. Please refer this article as- "Moisture effects on the bending fatigue of laminated composites", M. Meng; H. Le, S. Grove, M. J. Rizvi, Composite Structures, vol. 154, 15 October 2016, pp. 49-60. doi:10.1016/j.compstruct.2016.06.078
[URL: http://www.sciencedirect.com/science/article/pii/S0263822316310807]

where L_{3P} is the span for 3-point bending, L_{4P} is the outer span of the 4-point bending (the inner span is 1/3 of the outer span), w, h are the width and thickness of the laminate respectively, $F_{\max}/D_{\max}$ is the slope of the force-deflection, and $D_{\max}^{mid}$ is the deflection at the middle point of the specimen.

For the 4-point bending case, the maximum deflection shown in equation (2) was the deflection at the middle point of the laminate; however this is unavailable in the present work because the fatigue machine recorded the deflection at the loading point. Therefore, a formula was derived to determine the apparent flexural modulus from the deflection at the loading point (the derivation is shown in the Appendix),

$$E_{4P}^{f} = -\frac{23L^3}{104wh^3}\frac{F_{\max}}{D_{\max}^{load}} \qquad (3)$$

where $D_{\max}^{load}$ is the deflection at the loading point of the specimen.

The fatigue stiffness clearly shows the evolution of fatigue behaviour. Fig.6 shows the hysteresis loops of a cross-ply laminate under 3-point bending in terms of deflection-reaction force. Two loops were plotted in the figure, showing the histories at the beginning (100 cycles) and the end (5,000,000 cycles) of the test. The two loops almost overlapped each other, indicating that this type of plot can only provide limited information on the change of specimen state. Therefore the reaction force was transformed to flexural modulus by introducing the specimen dimension and bending condition, as shown in Fig.7. The two hysteresis loops illustrated the loading sequence within one single cycle as shown by the coloured arrows in the figure and the degradation of the flexural stiffness with increasing fatigue cycles.

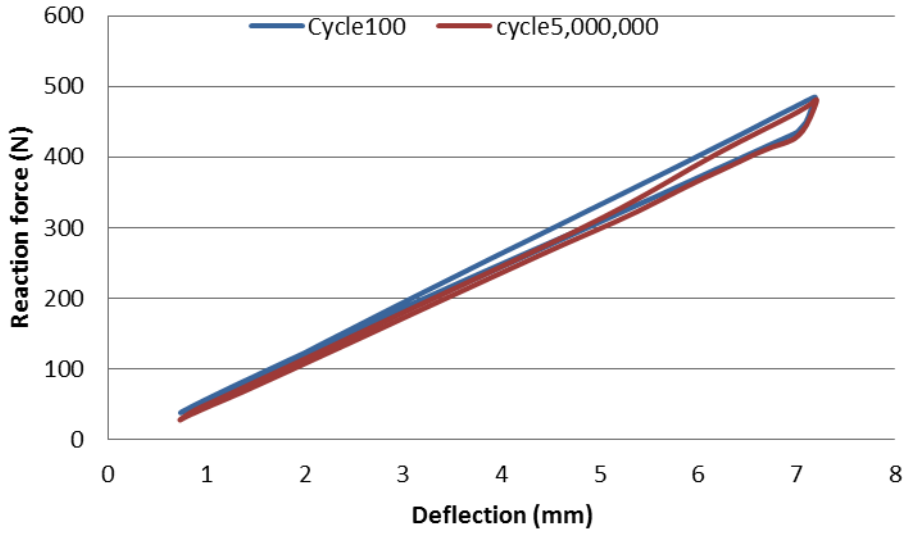

This article has been published in the Journal of Composite Structures. Please refer this article as- "Moisture effects on the bending fatigue of laminated composites", M. Meng; H. Le, S. Grove, M. J. Rizvi, Composite Structures, vol. 154, 15 October 2016, pp. 49-60. doi:10.1016/j.compstruct.2016.06.078
[URL: http://www.sciencedirect.com/science/article/pii/S0263822316310807]

Fig.6. Typical hysteresis loops of the deflection-reaction force of CP-dry laminate in 3-point bending fatigue test at the 80% UFS loading level

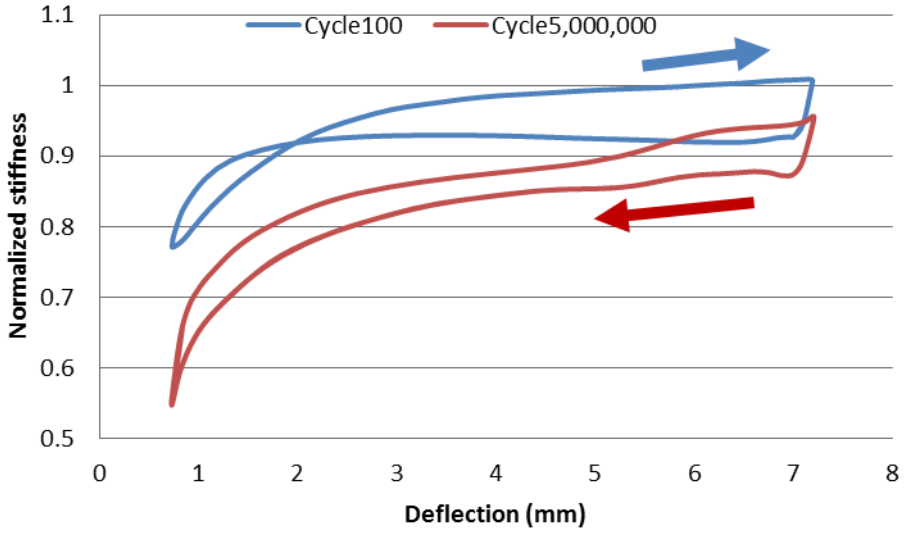

Fig.7. Typical hysteresis loops of the CP-dry laminate in 3-point bending fatigue test at the 80% UFS loading level in terms of normalized stiffness vs deflection. The stiffness was normalized relative to the dry condition. The directions of the hysteresis loops are also shown as arrows in the figure.

In terms of dynamic loading, the apparent reaction force is calculated by the sum of the specimen reaction and the acceleration of the load cell. In the sinusoidal cyclic loading, the acceleration decreases to zero at the maximum deflection and shifts to negative value when the load cell returns. Therefore, a sudden drop of the reaction force can be seen at the maximum deflection in Fig.6, and the amplified stiffness reduction from Fig.7. At the stage of minimum deflection, the flexural modulus decreased significantly from cycle 100 to cycle 5,000,000, as can be seen in the Fig.6, indicating fracture at the contact region on the compressive side. Additionally, based on the equation (3), the apparent flexural modulus at the minimum deflection was more sensitive to the deflection than at the maximum deflection.

Stiffness reduction was also observed in the 4-point bending fatigue test. A microscopic study of an 'infinite fatigue life' specimen, shown in Fig.8, reveals an explanation of this stiffness reduction at the minimum deflection observed in the fatigue test. First, the fracture initialized at the contact region between the load cell and the compressive surface of the specimen due to the stress concentration, showing a damaged interface. Later on some of the material in the pure bending region (between the two load rods) on the compressive surface was peeled off due to the compression and delamination. The stiffness decreased gradually when the specimen was peeled off ply by ply. As the fatigue test was force controlled, the deflection increased while the stiffness decreased. It should be noted that this was a very slow and continuous process; thus it is unacceptable to test the specimen till it fails, and it is reasonable

This article has been published in the Journal of Composite Structures. Please refer this article as- "Moisture effects on the bending fatigue of laminated composites", M. Meng; H. Le, S. Grove, M. J. Rizvi, Composite Structures, vol. 154, 15 October 2016, pp. 49-60. doi:10.1016/j.compstruct.2016.06.078
[URL: http://www.sciencedirect.com/science/article/pii/S0263822316310807]

to believe that the initial crack caused by contact or concentrated load is one important reason for fatigue failure of FRP composites.

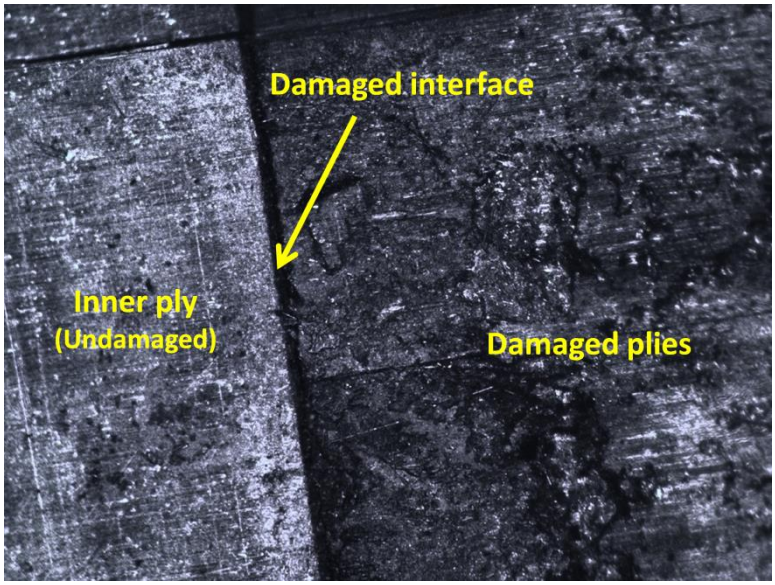

Fig.8. Typical fracture image of the CP laminate in 4-point bending fatigue test at the 80% UFS loading level. The specimen survived after withstanding more than five million cycles.

The fatigue failure of FRP composites is very complicated and is dependent on many aspects such as the testing conditions, environments, and the laminate layups, so that any attempt to predict the fatigue behaviour by a universal formulation may lead to inaccurate result. In the present work, the fatigue analysis of FRP composites in a marine environment is based on the study of the fatigue stiffness which shows a variety of interactions among the fatigue behaviour, laminate layups, testing conditions and the environmental effects.

The fatigue stiffness unveiled the effects of loading levels and the bending conditions, i.e. 3-point and 4-point bending. Fig.9 shows the flexural stiffness of cross-ply laminate without water immersion (CP-dry) tested in 3-point and 4-point bending. Both the specimens survived after withstanding more than 3×10^6 cycles at 80% UFS, and therefore were labelled as 'infinite fatigue life'. As can be seen from the figure, both the specimens showed nearly flat fatigue stiffness curves during the test cycles, demonstrating excellent fatigue performance at this loading level. However, the curve for the 4-point case showed a downward trend as the fatigue cycle increases, due to the contact and delamination shown in Fig.8. As a contrast, the curve of the 3-point case remained flat because the delamination at the contact region was constrained by the loading roller which prevented the propagation of the crack.

This article has been published in the Journal of Composite Structures. Please refer this article as- "Moisture effects on the bending fatigue of laminated composites", M. Meng; H. Le, S. Grove, M. J. Rizvi, Composite Structures, vol. 154, 15 October 2016, pp. 49-60. doi:10.1016/j.compstruct.2016.06.078
[URL: http://www.sciencedirect.com/science/article/pii/S0263822316310807]

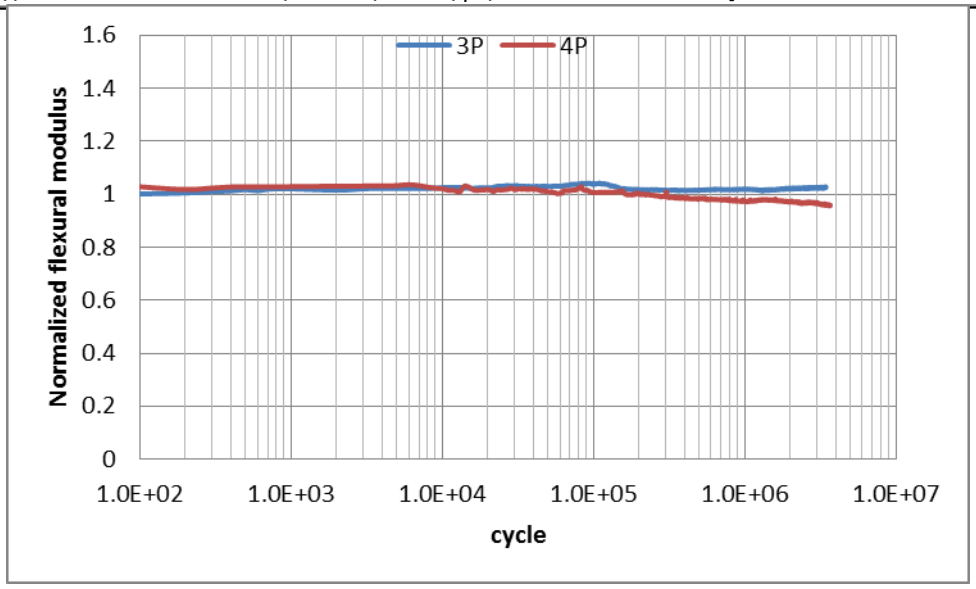

Fig.9. Typical fatigue stiffness of the CP-dry laminates with 'infinite fatigue life' in both 3-point and 4-point bending fatigue tests at the 80% UFS loading level. The fatigue stiffness was normalized to the flexural modulus which was tested in quasi-static bending.

For comparison, Fig.10 shows the 'broken' cases of the CP-dry laminates tested in 3-point and 4-point bending. Both the specimens were tested at 90% UFS. The 3-point case showed a flat fatigue stiffness which was similar with the 80% UFS case; however it failed suddenly when the damage accumulated to a critical value. The 4-point case presented a bigger stiffness reduction compared with the 80% UFS case (c.f. Fig. 9) until damaged plies accumulated to a critical value and then the specimen failed.

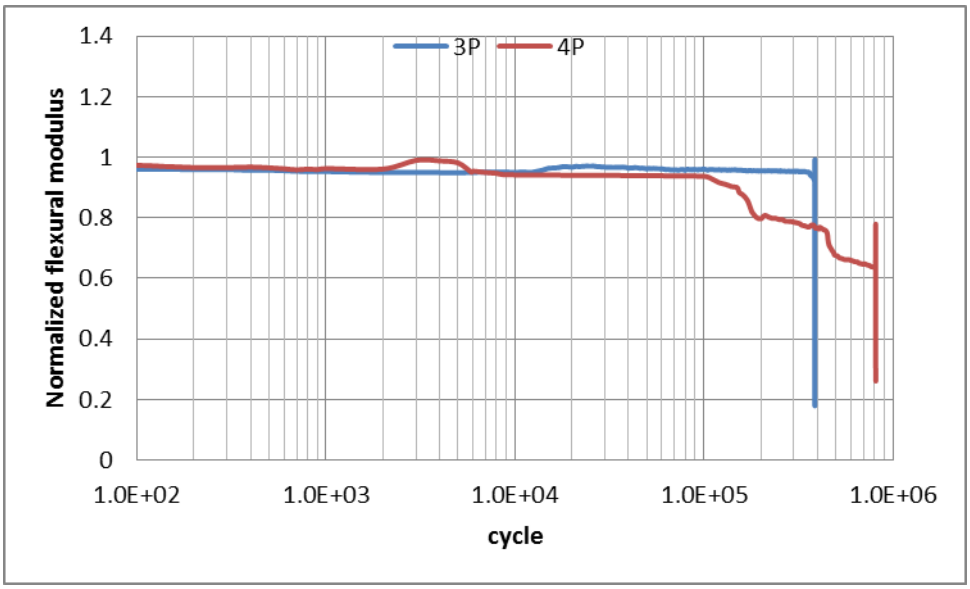

Fig.10. Typical fatigue stiffness of the CP-dry laminates in both 3-point and 4-point bending fatigue tests at 90% UFS loading level. Both the specimens failed.

This article has been published in the Journal of Composite Structures. Please refer this article as- "Moisture effects on the bending fatigue of laminated composites", M. Meng; H. Le, S. Grove, M. J. Rizvi, Composite Structures, vol. 154, 15 October 2016, pp. 49-60. doi:10.1016/j.compstruct.2016.06.078
[URL: http://www.sciencedirect.com/science/article/pii/S0263822316310807]

A similar trend can be seen in the fatigue stiffness of the UD-dry laminates, as shown in Fig.11. At 90% UFS, the specimen failed suddenly in 3-point bending due to fibre microbuckling which had been discussed in [13]. Both the specimens failed after withstanding more than 10^6 cycles. It is interesting to note that the UD specimen failed and broke into two pieces rapidly in 4-point quasi-static bending test, and the failure happened too quickly to be captured by a camera. However, in the fatigue test, the stiffness reduction, shown step by step, can be seen clearly, as well as the delamination on the compressive side of the specimen.

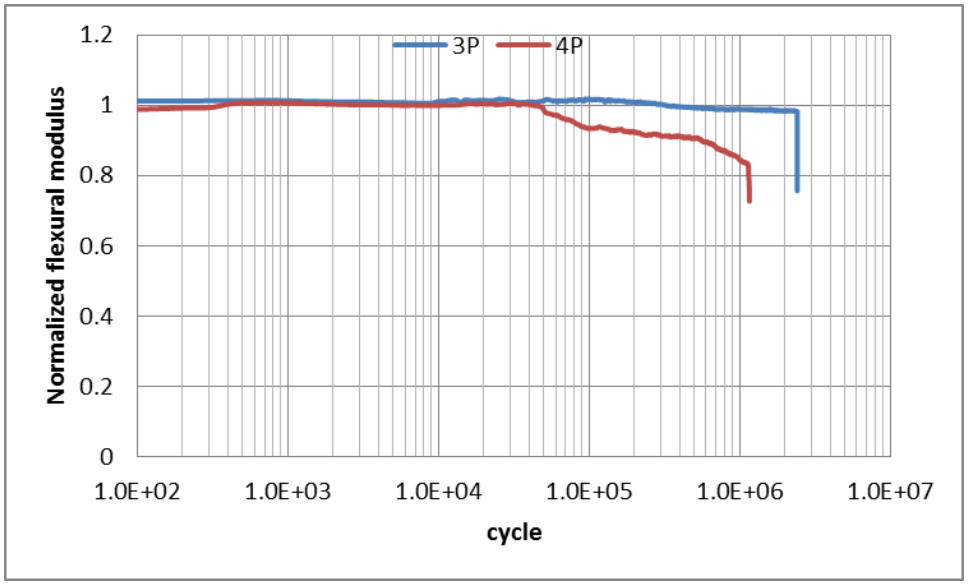

Fig.11. Typical fatigue stiffness of the UD-dry laminates in both 3-point and 4-point bending fatigue test at 90% UFS loading level

The effects of testing environments, i.e. dry and wet conditions, are shown in the fatigue stiffness results. Fig.12-13 show the comparison between the CP and UD laminates tested in dry and wet environments. There are three curves of fatigue stiffness in each figure for the comparison: (a) CP-dry-90%, dry specimen tested at 90% UFS which failed at the end of the test; (b) CP-tap-80%, tap water immersion specimen tested at 80% UFS which failed in the end of the test, and (c) CP-dry-80%, dry specimen tested at 80% UFS loading level which survived at the end of the test. No significant difference can be found from the testing environments of the tap water, sea water and sea water with 70 bar hydrostatic pressure.

As can be seen from Fig.12, the curves, as well as the fatigue failure modes, depend on the loading levels and the testing environments. The CP-dry-90% specimen failed and showed similar fatigue life with the CP-tap-80% specimen. However the previous one was tested at the highest loading level while the wet specimen was tested at 80% UFS. Hence, the water immersion degraded one level of the strength of FRP composites, and showed a reduction in both crack initiation time and failure times. On the other hand, no obvious stiffness reduction

This article has been published in the Journal of Composite Structures. Please refer this article as- "Moisture effects on the bending fatigue of laminated composites", M. Meng; H. Le, S. Grove, M. J. Rizvi, Composite Structures, vol. 154, 15 October 2016, pp. 49-60. doi:10.1016/j.compstruct.2016.06.078
[URL: http://www.sciencedirect.com/science/article/pii/S0263822316310807]

can be seen from the CP-tap-80% specimen until it failed suddenly when the damage accumulated to a critical value. This is different from the CP-dry-90% specimen which showed a step of approximate 10% stiffness reduction before it failed. The CP-dry-80% specimen survived to the end of the fatigue test although it showed a tiny stiffness reduction after about 2×10^6 cycles, which suggests that there is a cut off strength for this type of FRP composite in fatigue.

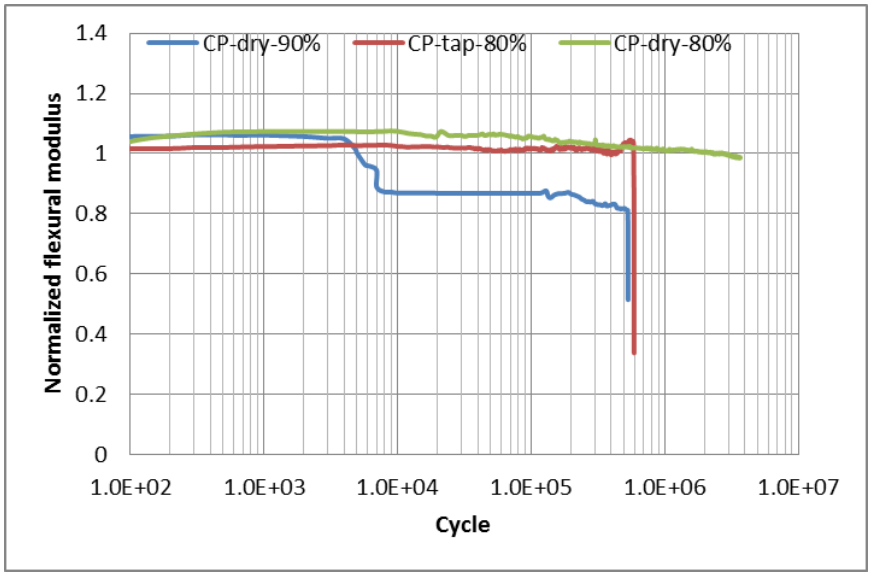

Fig.12. Typical fatigue stiffness of the CP laminates in 4-point bending fatigue test in dry and wet environments

The fatigue stiffness of UD laminates showed a similar trend although the failed specimens (UD-dry-90% and UD-tap-80%) withstood a higher fatigue cycle count. The comparison of the fatigue behaviour of these two layups demonstrates the high scatter of the composite fatigue behaviour. The observation that the fatigue failure process as well as the fatigue life of GFRP [26-28] and CFRP composites [29, 30] are accelerated by water immersion has been reported in the literature.

This article has been published in the Journal of Composite Structures. Please refer this article as- "Moisture effects on the bending fatigue of laminated composites", M. Meng; H. Le, S. Grove, M. J. Rizvi, Composite Structures, vol. 154, 15 October 2016, pp. 49-60. doi:10.1016/j.compstruct.2016.06.078
[URL: http://www.sciencedirect.com/science/article/pii/S0263822316310807]

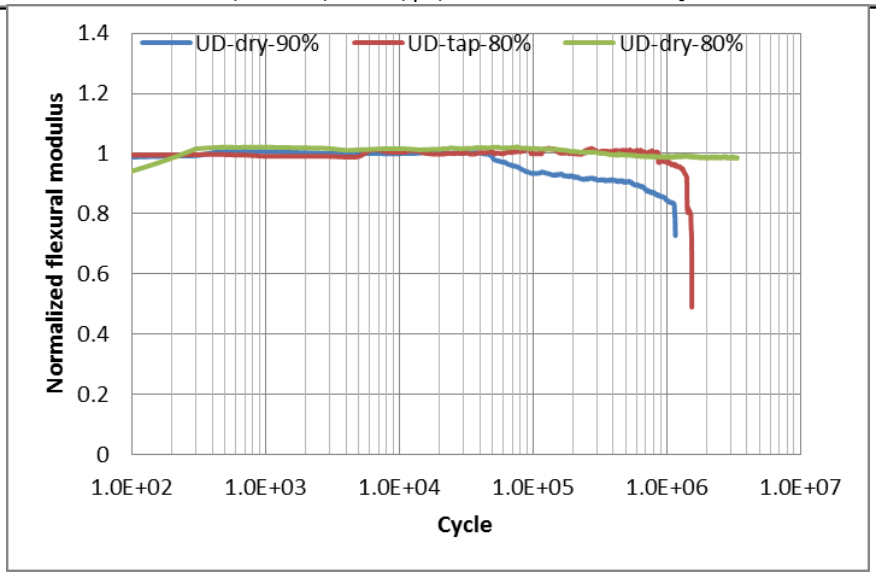

Fig.13. Typical fatigue stiffness of the UD laminates in 4-point bending fatigue in dry and wet environments

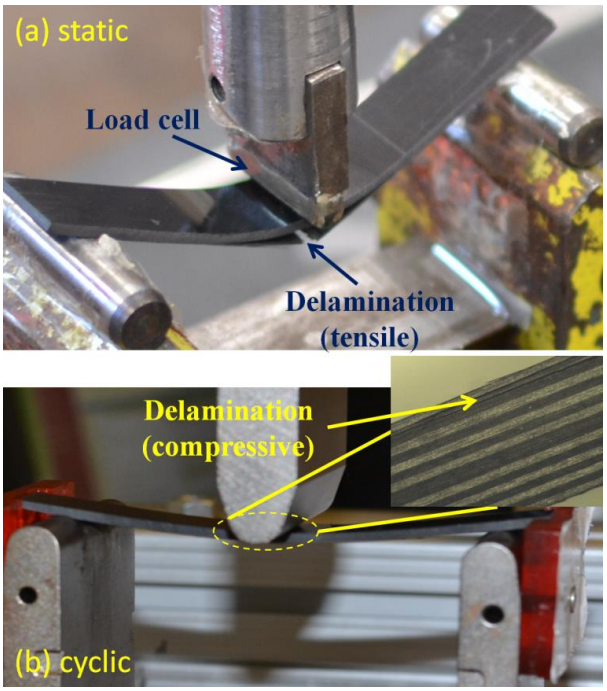

Fig.14. Comparison of the CP specimen failure mode in 4-point bending: (a) quasi-static bending and (b) bending fatigue

This article has been published in the Journal of Composite Structures. Please refer this article as- "Moisture effects on the bending fatigue of laminated composites", M. Meng; H. Le, S. Grove, M. J. Rizvi, Composite Structures, vol. 154, 15 October 2016, pp. 49-60. doi:10.1016/j.compstruct.2016.06.078
[URL: http://www.sciencedirect.com/science/article/pii/S0263822316310807]

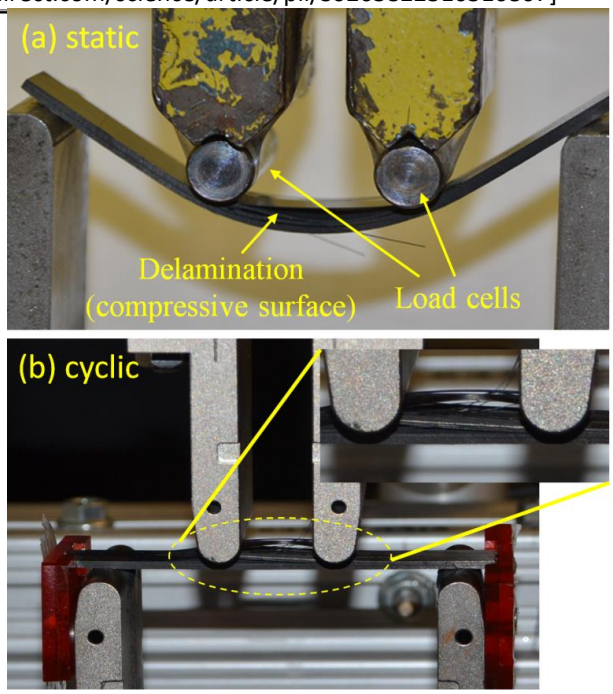

Fig.15. Comparison of the CP specimen failure mode in 4-point bending: (a) quasi-static bending and (b) bending fatigue

Experimental evidence shows the fatigue failure was also affected by the loading sequence, i.e. quasi-static and cyclic (fatigue) loading. Fig.14 and Fig.15 provide the evidence of different failure modes of the CP laminate associated with different testing conditions. In 3-point bending, as shown in Fig.14(a), the specimen failed by delamination caused by the maximum tensile stress at the bottom (tensile) surface. However, initial crack was found on the compressive surface of the CP specimen in the 3-point bending fatigue test, as shown in Fig. 14(b). This initial crack did not immediately lead to the failure of the laminate; instead, it accumulated, leading the applied stress to a critical value until the laminate failed rapidly, as shown in Fig.10.

Nevertheless, different failure modes were observed in 4-point bending. The specimens failed by delamination on the compressive surface regardless of the loading sequence (quasi-static or fatigue), as shown in Fig.16. This compressive delamination is regarded as buckling-driven delamination in the present work, which is discussed in the later section on the FEA modelling. It should be noted that, the compressive delamination failure was also observed in the UD specimen in the 4-point bending fatigue test. The UD specimen tested in 4-point quasi-static bending broke into two parts too rapidly to be observed by a camera; however the fracture surface indicated the crack initialized at the contact region on the compressive surface, as shown in Fig.16.

This article has been published in the Journal of Composite Structures. Please refer this article as- "Moisture effects on the bending fatigue of laminated composites", M. Meng; H. Le, S. Grove, M. J. Rizvi, Composite Structures, vol. 154, 15 October 2016, pp. 49-60. doi:10.1016/j.compstruct.2016.06.078
[URL: http://www.sciencedirect.com/science/article/pii/S0263822316310807]

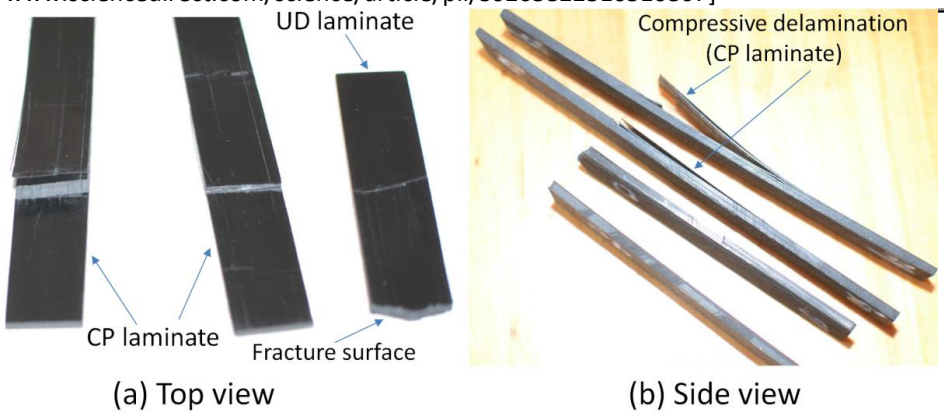

Fig.16. Typical failure modes of CP and UD laminates tested in 4-point quasi-static bending

4. FEA modelling

The experimental section had shown that compressive delamination was the main failure mode in bending fatigue. This is called buckling-driven delamination in the present work. A comparative study of the bending fatigue was conducted using FEA. Only the CP laminate was modelled for the study.

4.1 Virtual crack closure technique

VCCT uses linear elastic fracture mechanics (LEFM) concepts based on the strain energy release rate of the crack tip deformation, and compares the strain energy release rate to interlaminar fracture toughness [20]. For the pure mode I, as shown in Fig.17, nodes 2 and 5 will start to release when,

$$\frac{1}{2}\frac{v_{1,6}F_{v,2,5}}{wd} = G_I \geq G_{IC} \qquad (4)$$

where G_I and G_{IC} are mode I energy release rate and the critical energy release rate; w is the width; $F_{v,2,5}$ is the vertical force between nodes 2 and 5; $v_{1,6}$ is the vertical displacement between nodes 1 and 6. Mode II can be treated similarly.

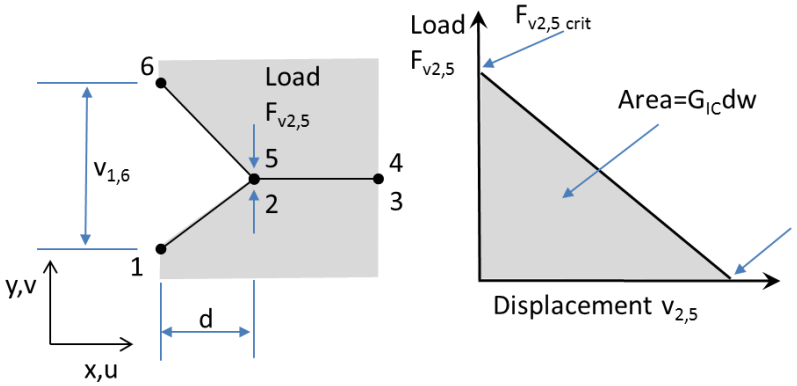

This article has been published in the Journal of Composite Structures. Please refer this article as- "Moisture effects on the bending fatigue of laminated composites", M. Meng; H. Le, S. Grove, M. J. Rizvi, Composite Structures, vol. 154, 15 October 2016, pp. 49-60. doi:10.1016/j.compstruct.2016.06.078
[URL: http://www.sciencedirect.com/science/article/pii/S0263822316310807]

Fig.17 Configuration of the virtual crack closure technique

The calculated G value must exceed the critical G_c before the crack propagates, and mixed mode propagation should be taken into account to evaluate the equivalent strain energy release rate. Compared with the power law, which requires three parameters corresponding to the three modes, the Benzeggagh-Kenane criterion, also known as BK law, is easier to implement,

$$G_{equivC} = G_{IC} + \left(G_{IIC} - G_{IIIC}\right)\left(\frac{G_{IIC} + G_{IIIC}}{G_{IC} + G_{IIC} + G_{IIIC}}\right)^{\eta} \quad (5)$$

where η is the BK law fitting parameter. The BK law was used in the present work for the FEA simulation.

The onset and fatigue delamination growth at the interfaces are characterized by using the Paris law, which relates crack growth rate da/dN to the relative strain energy release rate, as shown in Fig.18. The fatigue crack growth initiation criterion and the crack growth rate are defined as [31],

$$\frac{N}{c_1 \Delta G^{c_2}} \geq 1 \quad (6)$$
$$\Delta G = G_{max} - G_{min}$$

$$\frac{da}{dN} = c_3 \Delta G^{c_4} \quad (7)$$

where N is fatigue cycle; a is the crack length; c_1, c_2, c_3, c_4 are material constants; G_{max} and G_{min} correspond to the strain energy release rates when the structure is loaded up to F_{max} and F_{min} respectively.

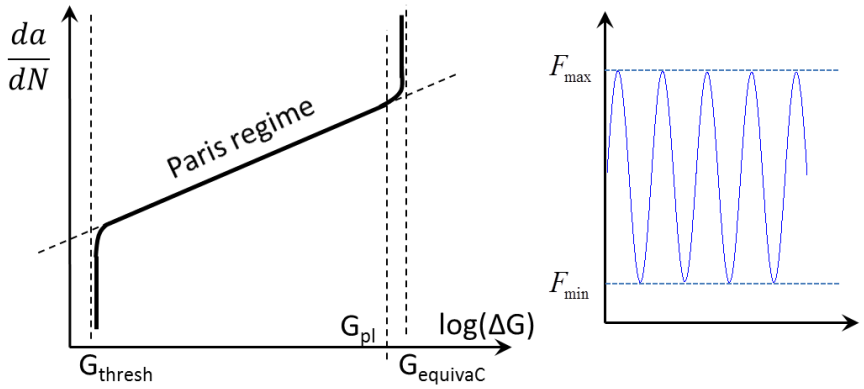

Fig.18. Schematics of fatigue crack growth relative to the Paris law. There is no fatigue crack initiation or growth when the strain energy release rate is lower than G_{thresh}.

This article has been published in the Journal of Composite Structures. Please refer this article as- "Moisture effects on the bending fatigue of laminated composites", M. Meng; H. Le, S. Grove, M. J. Rizvi, Composite Structures, vol. 154, 15 October 2016, pp. 49-60. doi:10.1016/j.compstruct.2016.06.078
[URL: http://www.sciencedirect.com/science/article/pii/S0263822316310807]

The interfacial elements at the crack tips will not be released unless the equation (6) and $G_{max}>G_{thresh}$ are satisfied and then the crack propagates initially quite rapidly until the so called Paris regime is reached where the growth rate reaches a steady rate. Once a critical crack length is reached, the crack will grow catastrophically when the G value is higher than the strain energy release rate upper limit G_{pl}. At this part final fast fracture occurs during the last fatigue cycle.

4.2 FEA implementation

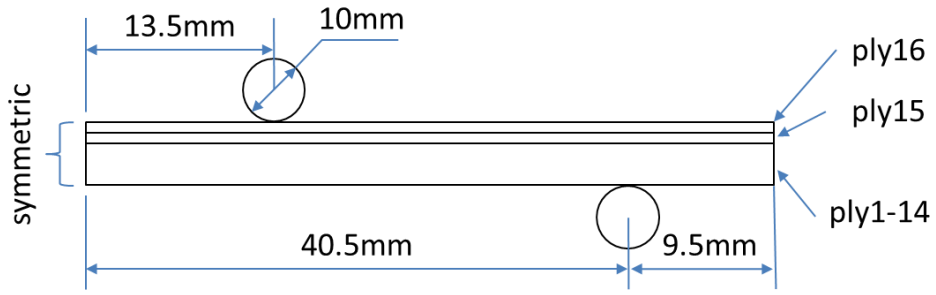

Fig.19. Schematics of the three layers FEA model

In 4-point bending, the cross-ply laminate is symmetric in geometry, material properties and the boundary condition, therefore the model was simplified to a half geometry and the crack was defined at the interface between ply15 (unidirectional transverse lamina, thickness 0.12mm) and ply16 (unidirectional lamina, thickness 0.12mm). The lower section ($[0/90]_{3s}90/0$, thickness 1.68mm), ply1-14 was considered as homogeneous orthotropic, whose material properties (flexural elastic properties) were calculated by CLT. Fig.19 illustrates the FEA model including three layers. The two rollers were considered as rigid body, and a contact boundary condition was applied for the interaction between the rollers and the specimen.

Table 3 Material properties for FEA simulation. The out-of-plane direction in 3D corresponds to the transverse direction in 2D model, i.e. $E_y=E_3$. For the comparison, the properties of the CP $[0/90]_{4s}$ laminate are also shown in the table.

Elastic properties					Fracture properties	
	ply16	ply15	ply1-14	$[0/90]_{4s}$	$G_{IC}(J/m^2)$	1500
E_x(GPa)	139	8.8	88	86	$G_{IIC}(J/m^2)$	1500
E_y(GPa)	8.8	8.8	11	11	$G_{IIIC}(J/m^2)$	1500
ν_{xy}(GPa)	0.26	0.02	0.04	0.04	*η	1.75
ν_{yz}(GPa)	0.48	0.26	0.44	0.43	c_1	0.5
ν_{xz}(GPa)	0.26	0.48	0.41	0.41	c_2	-0.1
G_{xy}(GPa)	4.7	4.7	4.7	4.7	c_3	4.88E-06
G_{xz}(GPa)	4.7	3	4	4	c_4	1.15

This article has been published in the Journal of Composite Structures. Please refer this article as- "Moisture effects on the bending fatigue of laminated composites", M. Meng; H. Le, S. Grove, M. J. Rizvi, Composite Structures, vol. 154, 15 October 2016, pp. 49-60. doi:10.1016/j.compstruct.2016.06.078
[URL: http://www.sciencedirect.com/science/article/pii/S0263822316310807]

***The fitting parameter η for BK law and the four parameters $c_{1,2,3,4}$ for Paris law were estimated based on reference [31].**

According to the open literature [32, 33], the critical strain energy release rates of 977-2 epoxy based composites are in the range of 600-2400 J/m^2. Therefore, an intermediate value, G_c=1500 J/m^2 was applied on the FEA model. Table 3 gives the material information, including elastic and fracture properties.

For VCCT, an initial crack must be embedded into the interfacial elements and the crack path should be defined. It is reasonable to assume that the crack was initiated under the load roller due to the stress concentration here. According to the 3D solid modelling of quasi-static bending [13], the solution was mesh independent when each ply was divided into three elements through thickness, however the contact region should be refined to capture the stress concentration due to the contact. For the fatigue modelling, the loading history was simplified as triangular function instead of the sinusoidal shape. Fig.20 plots the mesh of the FEA model and the schematics of loading history. The FEA model was solved by ABAQUS/Standard (Version 6.14).

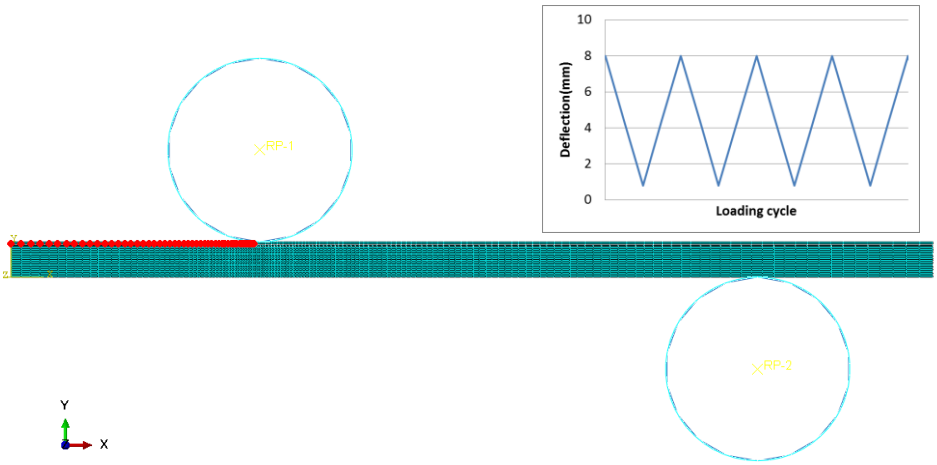

Fig.20. Mesh plot of the three layer FEA model and the loading history. An initial crack (0.2mm) was embedded at the interface between ply15 and ply16 under the load roller. The crack path (shown as red dots) is also shown in the figure.

It should be noted that the maximum deflection had exceeded the 'large-deflection criterion'; therefore nonlinear behaviour must be taken into account. Fig.21 presents the stress distribution of the whole model. The buckling-driven delamination is clearly shown. Due to the limit of the current FEA technique, multiple cracks are not allowed to cross each other; therefore ply16 still withstood part of the compressive stress and the stiffness reduction was not as significant as observed in the specimen after buckling.

Fig.22 compares the flexural force-deflection curves for the three cases. For the case (a), FEA simulation without initial crack, the reaction force increased with the increase of deflection

This article has been published in the Journal of Composite Structures. Please refer this article as- "Moisture effects on the bending fatigue of laminated composites", M. Meng; H. Le, S. Grove, M. J. Rizvi, Composite Structures, vol. 154, 15 October 2016, pp. 49-60. doi:10.1016/j.compstruct.2016.06.078
[URL: http://www.sciencedirect.com/science/article/pii/S0263822316310807]

and the curve showed a linear relation until the deflection was close to about 10% of the bending span (large deflection criterion). According to the CLT formulae, the apparent flexural modulus of the CP laminate ($[0/90]_{4S}$) is calculated as 86 GPa, which is slightly higher than the experimental data (measured as 80 GPa), therefore the reaction force in the FEA simulation showed a higher value than the experiment at the same deflection. For the case (b), FEA simulation with 0.2mm initial crack, the curve showed a zigzag aspect at the linear stage indicating the debonding of the interfacial elements. With the growth of the crack length and the increase of deflection as well as the compressive stress, the part of ply16 above the crack buckled when the loading was increased to approximately 90% of the ultimate flexural strength, leading to a sudden delamination, therefore the curve showed a significant oscillation. In FEA, ply16 still withstood compressive stress after it buckled; therefore the stiffness was relatively high. As a contrast, (c) the experiment observation showed that ply16 failed after it buckled and the stiffness reduced significantly.

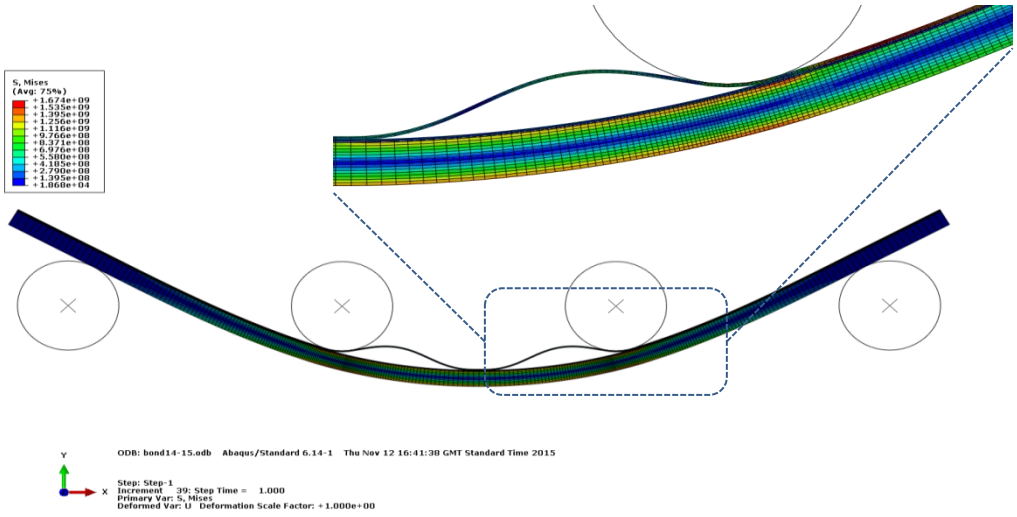

Fig.21. Distribution of stress. A magnified view of the delamination is also shown in the figure.

This article has been published in the Journal of Composite Structures. Please refer this article as- "Moisture effects on the bending fatigue of laminated composites", M. Meng; H. Le, S. Grove, M. J. Rizvi, Composite Structures, vol. 154, 15 October 2016, pp. 49-60. doi:10.1016/j.compstruct.2016.06.078
[URL: http://www.sciencedirect.com/science/article/pii/S0263822316310807]

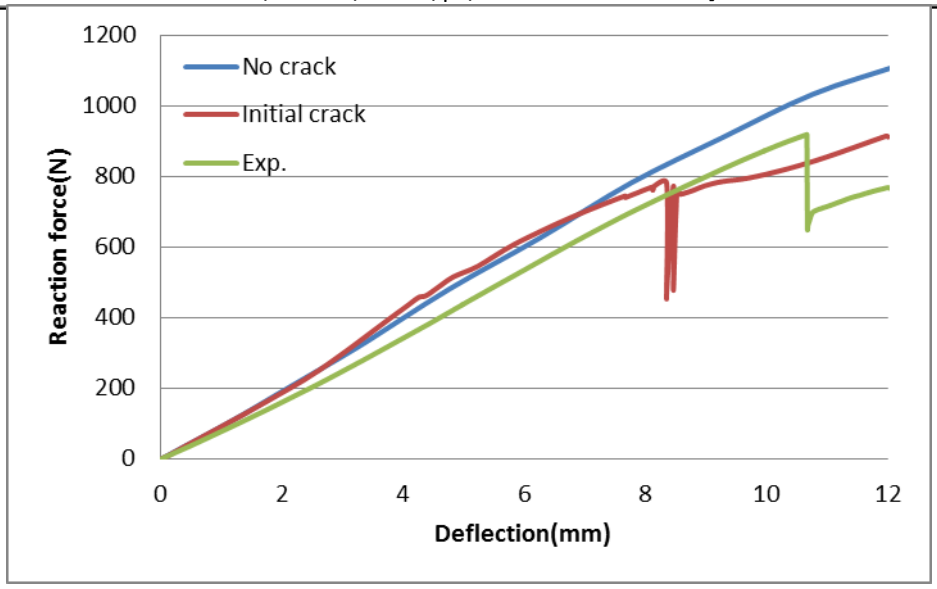

Fig.22. Relation between reaction force and deflection for three cases: (a) FEA simulation without initial crack; (b) FEA simulation with 0.2mm initial crack; and (c) a typical experimental curve of CP-dry specimen.

Figs.23 and 24 present the distributions of mode I and mode II strain energy release rates along the crack path at the moments of the onset of buckling and after sudden delamination. It is apparent that the crack propagated in a single direction due to the constraint of the load cell. It can be seen from Fig.23 that the onset of buckling was associated with mode I; however the mode I strain energy release rate reduced exponentially when the buckling initiated; after that the delamination was driven by mode II according to Fig.24. Therefore, the onset of the buckling was mode I dominated while the crack propagation was mode II dominated.

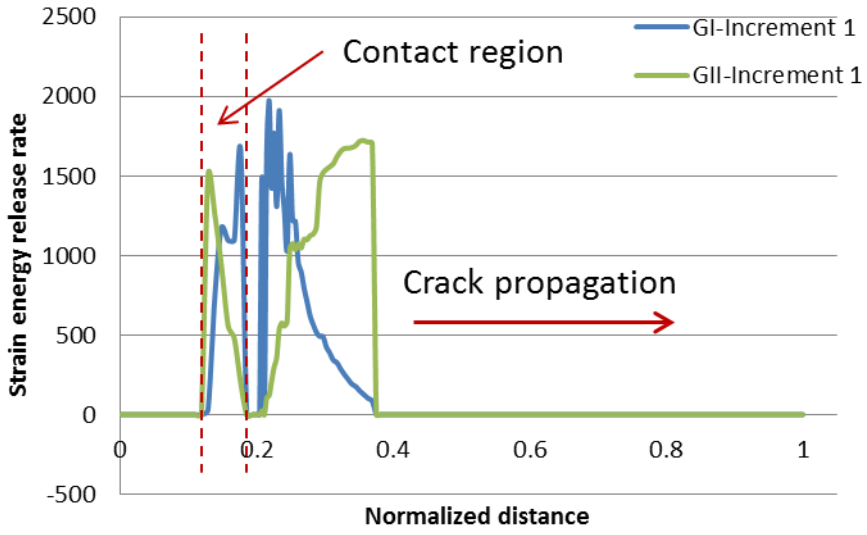

This article has been published in the Journal of Composite Structures. Please refer this article as- "Moisture effects on the bending fatigue of laminated composites", M. Meng; H. Le, S. Grove, M. J. Rizvi, Composite Structures, vol. 154, 15 October 2016, pp. 49-60. doi:10.1016/j.compstruct.2016.06.078
[URL: http://www.sciencedirect.com/science/article/pii/S0263822316310807]

Fig.23. Distributions of mode I and mode II strain energy release rates along the crack path when the buckling initialized. The crack path was normalized.

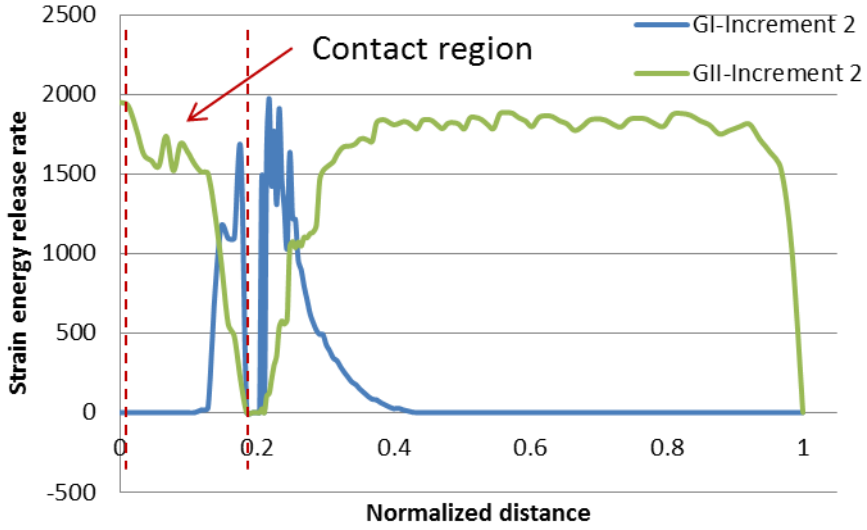

Fig.24. Distributions of mode I and mode II strain energy release rates along the crack path after the catastrophic delamination. The contact region enlarged due to the tangential slide of the specimen/load cell and the buckling deformation of ply16.

It was observed that the initial crack length has no effect on when the buckling happens if it is shorter than a critical length. Once the buckling was initialized, the crack propagated rapidly in FEA. The parametric study on the critical strain energy release rate showed that the buckling was initiated at a larger deflection at higher critical strain energy release rate. However the deflection at buckling was not as large as that in the experiment due to the artificial initial crack in the FEA. Therefore, the initial crack must be critical to the flexural strength and the fatigue life. Since the initial crack is caused by the stress concentration, the apparent flexural strength is expected to be significantly higher if the stress concentration is reduced, for instance, by increasing the radius of the load arm.

Recalling the fatigue stiffness of CP specimen in Fig.10, the initial crack was induced by the stress concentration at relatively low cycle count at the highest loading level. Since this loading level was very close to the buckling criterion shown in Fig.22, ply16 failed by the buckling-driven delamination rapidly, corresponding to the stiffness reduction shown in Fig.10. Since the onset of the buckling is associated with the mode I strain energy release rate, this may lead to an assumption that those FRP composites with higher mode I strain energy release rate are expected to achieve better fatigue life at high loading levels.

This article has been published in the Journal of Composite Structures. Please refer this article as- "Moisture effects on the bending fatigue of laminated composites", M. Meng; H. Le, S. Grove, M. J. Rizvi, Composite Structures, vol. 154, 15 October 2016, pp. 49-60. doi:10.1016/j.compstruct.2016.06.078
[URL: http://www.sciencedirect.com/science/article/pii/S0263822316310807]

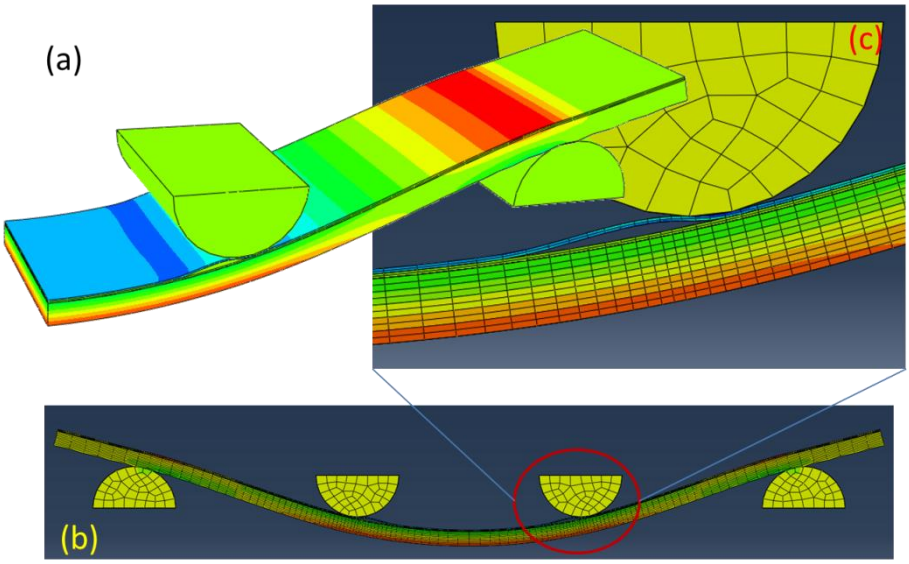

Fig.24 Distribution of longitudinal stress component (s11) of the 3D solid FEA model: (a) isotropic view; (b) side view; and (c) a magnified side view.

The 2D FEA model has loss the transverse information; therefore a comprehensive 3D solid model was built to compare with the 2D model. The 3D solid model was similar to the 2D containing three-layer structure. Taking advantage of the symmetry it is sufficient to consider a quarter of the region. The 3D FEA model suffered convergent problem if the load roller was defined as rigid body, therefore they were designated as steel. The mesh near the transverse edge was refined in order to capture the edge effect. Due to the limit of the computing resource, the through-thickness mesh of ply15 and ply16 was only divided into two layers. Fig.24 shows the similar buckling-driven delamination to the 2D model.

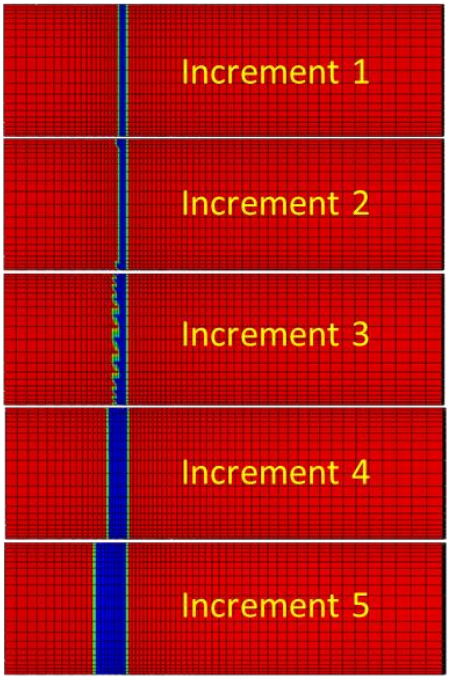

This article has been published in the Journal of Composite Structures. Please refer this article as- "Moisture effects on the bending fatigue of laminated composites", M. Meng; H. Le, S. Grove, M. J. Rizvi, Composite Structures, vol. 154, 15 October 2016, pp. 49-60. doi:10.1016/j.compstruct.2016.06.078
[URL: http://www.sciencedirect.com/science/article/pii/S0263822316310807]

Fig.25 Bonding state of the interfacial elements as the fatigue crack propagating (top view). The blue elements denote debonding while the red elements denote bonding.

Fig.25 presents the progressive debonding of the 3D solid model. Although an initial crack was embedded underneath the load roller, it was found that the foregoing debonding elements were formed at the edge during the fatigue crack propagation, as shown in increment 2, and then the crack propagated through the transverse direction, as shown in increment 3. For an intact specimen in experiment, it is reasonable to state that the crack is induced at the two edges underneath the load roller by the combination of the stress concentration and edge effect.

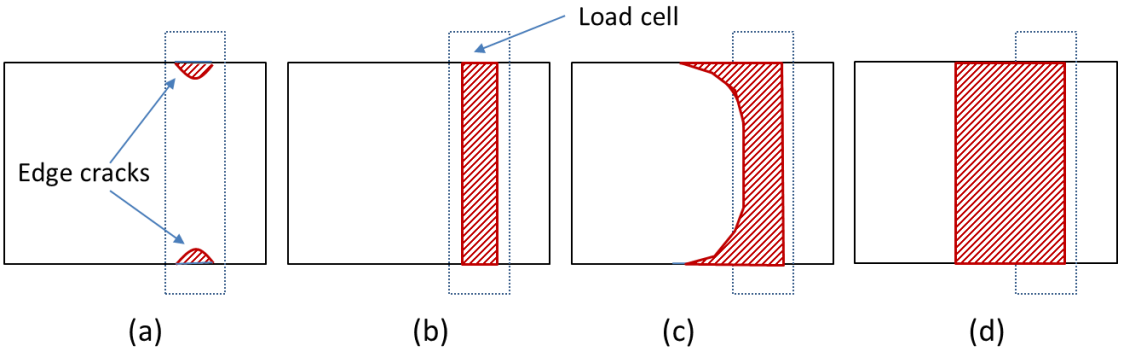

Fig.26 Development of buckling-driven delamination in bending fatigue: (a) edge cracks initialized; (b) edge cracks penetrated through width; (c) foregoing edge cracks; (d) compressive ply buckled and buckling-driven delamination

Therefore, it is inferred that the buckling-driven delamination in fatigue was comprised four steps, as shown in Fig.26: (a) the edge cracks were induced underneath the load cell; (b) the edge cracks penetrated inside the laminate to form the initial crack (which was embedded in the FEA model); (c) the edge cracks lead the forgoing fracture during the fatigue; until (d) the crack length met the criterion of buckling and then the buckling drove a catastrophic delamination. After the first compressive ply (top surface) failed by the buckling-driven delamination, the second ply repeated the same process, and then the third ply (as shown in Fig.8) … until the whole specimen failed.

In case of those specimens fatigue tested in the wet environment (i.e. covered by a wet sponge), it is apparent that water climbed into the cracks due to the capillary effect. Smith and Weitsman used X-ray to investigate the capillary effect of the immersed fatigue response of CFRP composites and found that the rate of capillary climb was approximately 7mm/min regardless of stress levels [34]. Compared with the moisture diffusivity of polymer composites, the rate of capillary climb is one million times faster; therefore it is reasonable to assume that the foregoing mass of water is preserved during the loading cycle. As a consequence, the water prevented the crack closure when the specimen was unloaded, and then the crack propagation was accelerated, leading to a much shorter fatigue life.

This article has been published in the Journal of Composite Structures. Please refer this article as- "Moisture effects on the bending fatigue of laminated composites", M. Meng; H. Le, S. Grove, M. J. Rizvi, Composite Structures, vol. 154, 15 October 2016, pp. 49-60. doi:10.1016/j.compstruct.2016.06.078
[URL: http://www.sciencedirect.com/science/article/pii/S0263822316310807]

5. Conclusions

Following diffusion measurements [5, 13], this paper performed the fatigue studies of dry and saturated laminate specimens (tap water immersion, sea water immersion, and sea water immersion with 70bar hydrostatic pressure) in both dry and wet environments. Bending fatigue (both 3-point and 4-point bending) tests were carried out at three loading levels to investigate the fatigue performance of the UD and CP laminates. FEA modelling, based on VCCT, investigated the fatigue crack propagation as well as the fatigue failure mechanisms.

The UD and CP laminates showed different fatigue failure behaviour but a similar response to environmental effects. It was found that the water degradation reduced the fatigue performance: dry specimens survived at 80% UFS but failed at 90%UFS, while water conditioned coupons survived at 65%UFS by failed at 80%UFS. However, no evidence was found to identify the different effects of the three immersions on the fatigue performance.

Water ingress during fatigue significantly accelerated the crack initiation and fatigue crack propagation, therefore a short fatigue life was expected. Experimental observation showed that the immersed coupons failed when tested in wet environment (80% UFS) but survived when tested in air at the same loading level.

The traditional SN curve was inappropriate to predict the fatigue of CFRP composites and the fatigue analysis must be associated with the loading conditions. The study of the fatigue stiffness has shown that the fatigue failure modes were associated with bending condition (3-point and 4-point bending), loading level, loading sequence, stacking sequence and the loading environments (dry and wet). Any attempt to analyse the fatigue failure mechanisms without consideration of the practical conditions will lead to inaccurate results.

Both the UD and CP laminates failed by buckling-driven delamination in 4-point bending fatigue. FEA based on VCCT simulated the buckling-driven delamination in both 2D and 3D. It was found that the initiation of buckling was mode I dominated while the fatigue crack propagation was mode II dominated.

FEA modelling unveiled the development of the 4-step buckling-driven delamination, in which the edge effect played an important role in the fatigue crack propagation. Furthermore, the water ingress due to the capillary phenomenon significantly accelerated the progress of crack initiation and propagation.

6. Acknowledgments

The authors would like to thank Dr Richard Cullen for his kind help with composites manufacturing, Terry Richards for his support of the mechanical tests, Dr Alistair Cree for his kind comments, and the financial support of the School of Marine Science and Engineering, Plymouth University.

This article has been published in the Journal of Composite Structures. Please refer this article as- "Moisture effects on the bending fatigue of laminated composites", M. Meng; H. Le, S. Grove, M. J. Rizvi, Composite Structures, vol. 154, 15 October 2016, pp. 49-60. doi:10.1016/j.compstruct.2016.06.078
[URL: http://www.sciencedirect.com/science/article/pii/S0263822316310807]

7. Reference

1. Mohan, M., *The advantages of composite materials in marine renewable energy structures.* RINA Marine Renewable Energy Conference 2008 2008.
2. SIEMENS, *www.siemens.com.* 2008.
3. Hammerfest, A.H., *www.hammerfeststrom.com.* 2011.
4. Meng, M., et al., *Multi-scale modelling of moisture diffusion coupled with stress distribution in CFRP laminated composites.* Composite Structures, 2016. **138**: p. 295-304.
5. Meng, M., et al., *Effects of hygrothermal stress on the failure of CFRP composites.* Composite Structures, 2015. **133**: p. 1024-1035.
6. Hashin, Z., *Fatigue failure criteria for unidirectional fiber composites.* Journal of Applied Mechanics, 1981. **48**(4): p. 846-852.
7. Epaarachchi, J.A. and P.D. Clausen, *An empirical model for fatigue behavior prediction of glass fibre-reinforced plastic composites for various stress ratios and test frequencies.* Composites Part A: Applied science and manufacturing, 2003. **34**(4): p. 313-326.
8. Reis, P., et al., *Fatigue life evaluation for carbon/epoxy laminate composites under constant and variable block loading.* Composites Science and Technology, 2009. **69**(2): p. 154-160.
9. Norwood, L. and A. Marchant, *Recent developments in polyester matrices and reinforcements for marine applications, in particular polyester/kevlar composites*, in *Composite structures*. 1981, Springer. p. 158-181.
10. Wood, C.A. and W.L. Bradley, *Determination of the effect of seawater on the interfacial strength of an interlayer E-glass/graphite/epoxy composite by in situ observation of transverse cracking in an environmental SEM.* Composites science and Technology, 1997. **57**(8): p. 1033-1043.
11. Juska, T., *Effect of water immersion on fiber/matrix adhesion*. 1993, DTIC Document.
12. Juska, T., *Effect of water immersion on fiber/matrix adhesion in thermoplastic composites.* Journal of Thermoplastic Composite Materials, 1993. **6**(4): p. 256-274.
13. Meng, M., et al., *3D FEA modelling of laminated composites in bending and their failure mechanisms.* Composite Structures, 2015. **119**(0): p. 693-708.
14. Melenk, J.M. and I. Babuška, *The partition of unity finite element method: Basic theory and applications.* Computer Methods in Applied Mechanics and Engineering, 1996. **139**(1–4): p. 289-314.
15. Abdelaziz, Y. and A. Hamouine, *A survey of the extended finite element.* Computers & Structures, 2008. **86**(11–12): p. 1141-1151.
16. Belytschko, T., R. Gracie, and G. Ventura, *A review of extended/generalized finite element methods for material modeling.* Modelling and Simulation in Materials Science and Engineering, 2009. **17**(4): p. 043001.
17. Park, K. and G.H. Paulino, *Cohesive zone models: a critical review of traction-separation relationships across fracture surfaces.* Applied Mechanics Reviews, 2011. **64**(6): p. 060802.
18. Chowdhury, S.R. and R. Narasimhan, *A cohesive finite element formulation for modelling fracture and delamination in solids.* Sadhana, 2000. **25**(6): p. 561-587.
19. Irwin, G.R., *Analysis of stresses and strains near the end of a crack traversing a plate.* SPIE MILESTONE SERIES MS, 1997. **137**: p. 167-170.
20. Rybicki, E.F. and M. Kanninen, *A finite element calculation of stress intensity factors by a modified crack closure integral.* Engineering Fracture Mechanics, 1977. **9**(4): p. 931-938.
21. Raju, I., *Calculation of strain-energy release rates with higher order and singular finite elements.* Engineering Fracture Mechanics, 1987. **28**(3): p. 251-274.
22. ISO14125, *Fibre-reinforced plastic composites— Determination of flexural properties*, in *ISO standard*. 1998.
23. ISO13003, *13003. Fibre-reinforced plastics–determination of fatigue properties under cyclic loading conditions.* British Standards International, 2003.

24. D5229, A., *Standard test method for moisture absorption properties and equilibrium condition of polymer matrix composite materials*. 2004.
25. Peters, S.T., *Handbook of composites*. 2013: Springer Science & Business Media.
26. Boller, K., *Fatigue characteristics of RP laminates subjected to axial loading.* Modern Plastics, 1964. **41**(10): p. 145-150.
27. Phillips, D., J. Scott, and N. Buckley, *The effects of moisture on the shear fatigue of fibre composites.* ICCM/2, 1978: p. 1544-1559.
28. Yang, B.-X., M. Kasamori, and T. Yamamoto. *The effect of water on the interlamina delamination growth of composite laminates*. in *The Second International Symposium on Composite Materials and Structures*. 1992.
29. Morton, J., S. Kellas, and S. Bishop, *Damage characteristics in notched carbon fiber composites subjected to fatigue loading—Environmental effects.* Journal of composite materials, 1988. **22**(7): p. 657-673.
30. Sumsion, H., *Environmental effects on graphite-epoxy fatigue properties.* Journal of Spacecraft and Rockets, 1976. **13**(3): p. 150-155.
31. ABAQUS, *ABAQUS reference manual.* 2015.
32. Liu, S. and J.A. Nairn, *The formation and propagation of matrix microcracks in cross-ply laminates during static loading.* Journal of reinforced plastics and composites, 1992. **11**(2): p. 158-178.
33. Hottengada, B., *Investigation of Microcracking and Damage Propagation in Cross-Ply Composite Laminates.* 2006.
34. Smith, L. and Y. Weitsman, *The immersed fatigue response of polymer composites.* International journal of fracture, 1990. **82**(1): p. 31-42.

This article has been published in the Journal of Composite Structures. Please refer this article as- "Moisture effects on the bending fatigue of laminated composites", M. Meng; H. Le, S. Grove, M. J. Rizvi, Composite Structures, vol. 154, 15 October 2016, pp. 49-60. doi:10.1016/j.compstruct.2016.06.078
[URL: http://www.sciencedirect.com/science/article/pii/S0263822316310807]

Appendix

Considering an Euler beam under 4-point bending condition, the inner span is one third of the outer span, as shown in Fig.A.

At the zone AB, the moment is expressed as,

$$M = E_{4P}^{f} Iy'' = \frac{1}{2} Fx, 0 \le x \le \frac{L}{3} \qquad \text{(A1)}$$

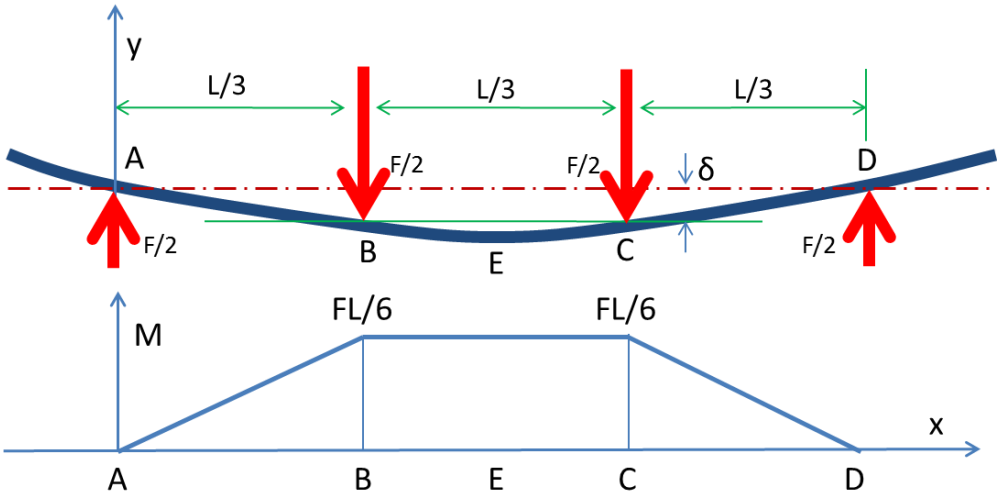

Fig.A. Schematics of 4-point bending and the distribution of moment

Integrating equation (A1) twice,

$$E_{4P}^{f} Iy' = \frac{1}{4} Fx^2 + C_1, E_{4P}^{f} Iy_B^{'} = \frac{1}{36} FL^2 + C_1$$
$$E_{4P}^{f} Iy = \frac{1}{12} Fx^3 + C_1 x + C_2, E_{4P}^{f} Iy_A = 0, C_2 = 0 \qquad \text{(A2)}$$
$$E_{4P}^{f} Iy_B = \frac{1}{324} FL^3 + \frac{1}{3} C_1 L$$

where I is the moment of inertia, y_B, y_E are the deflections at the loading point and middle point respectively.

At the zone BC, the moment is expressed as,

$$M = E_{4P}^{f} Iy'' = \frac{1}{6} FL, \frac{L}{3} \le x \le \frac{2L}{3} \qquad \text{(A3)}$$

Integrating equation (A3),

This article has been published in the Journal of Composite Structures. Please refer this article as- "Moisture effects on the bending fatigue of laminated composites", M. Meng; H. Le, S. Grove, M. J. Rizvi, Composite Structures, vol. 154, 15 October 2016, pp. 49-60. doi:10.1016/j.compstruct.2016.06.078
[URL: http://www.sciencedirect.com/science/article/pii/S0263822316310807]

$$E_{4P}^{f} Iy' = \frac{1}{6} FLx + C_3 \tag{A4}$$

The differential at the middle point is zero, leading to $y_E^{'} = 0$. Therefore,

$$\begin{aligned} E_{4P}^{f} Iy_E^{'} &= \frac{1}{12} FL^2 + C_3 = 0, C_3 = -\frac{1}{12} FL^2 \\ E_{4P}^{f} Iy_B^{'} &= -\frac{1}{36} FL^3 \end{aligned} \tag{A5}$$

Integrating equation (A5),

$$\begin{aligned} E_{4P}^{f} Iy &= \frac{1}{12} FLx^2 + \frac{1}{12} FL^2 x + C_4 \\ E_{4P}^{f} Iy_B &= \frac{1}{54} FL^3 + C_4 \end{aligned} \tag{A6}$$

Combining equations (A2) and (A6),

$$C_1 = -\frac{1}{18} FL^2, C_4 = \frac{1}{324} FL^3 \tag{A7}$$

Substituting the equation (A7) and the inertia of moment $I = \frac{1}{12} wh^3$ into equations (A5) and (A6), the flexural moduli at the loading point and mid-point are then calculated by,

$$E_{4P}^{f} = -\frac{5L^3}{27wh^3} \frac{F}{y_B} \tag{A8-1}$$

$$E_{4P}^{f} = -\frac{23L^3}{104wh^3} \frac{F}{y_E} \tag{A8-2}$$

The equation (A8-2) is the same as the one in the ISO standard shown as equation (2) using the deflection at the middle point.